Research Article

Anti-Inflammatory and Antioxidant Properties of *Physalis alkekengi* L. Extracts *In Vitro* and *In Vivo*: Potential Application for Skin Care

Bing-Wei He [iD],[1,2] **Fei-Fei Wang** [iD],[1,2,3] and **Li-Ping Qu** [iD][1,2,3]

[1]*Yunnan Botanee Bio-technology Group Co., Ltd., Yunnan 650106, China*
[2]*Yunnan Yunke Characteristic Plant Extraction Laboratory Co., Ltd., Yunnan 650106, China*
[3]*Shanghai Jiyan Bio-pharmaceutical Co., Ltd., Shanghai 201702, China*

Correspondence should be addressed to Li-Ping Qu; quliping@winona.cn

Objective. Inflammatory skin disorders are becoming major issues threatening public health with increasing prevalence. This study was to evaluate the anti-inflammatory, antioxidant, and antisenescent activities of traditional folk medicinal plant, *Physalis alkekengi* L. extracts to alleviate skin inflammation and its possible mechanisms. *Methods.* Lipopolysaccharides (LPS)-treated murine macrophages RAW264.7 and human skin keratinocytes HaCaT were incubated with the plant extracts, respectively. The production of nitric oxide (NO) was tested by using Griess reagents. The activity of nitric oxide synthase (NOS) was detected through a fluorescence microplate reader. Reactive oxygen species (ROS) production and cell apoptosis were quantified by flow cytometry. The proinflammatory cytokines were measured using ELISA and qRT-PCR. Human skin fibroblasts (HFF-1) were coincubated with D-galactose (D-gal) and the plant extracts. The senescence associated-galactosidase (SA-β-gal) was stained to evaluate cellular senescence. The senescence-associated secretory phenotype (SASP), IL-1β, was measured through ELISA. The mRNA of IL-1α in SLS-stimulated and PGE2 in UV-radiated 3D skin models were detected by qRT-PCR. *In vivo* ROS production and neutrophil recruitment in CuSO$_4$-treated zebrafish models were observed by fluorescence microscopy. Inflammation-related factors were measured by qRT-PCR. *Results. In vitro*, *Physalis alkekengi* L. significantly reduced NO production, NOS activity, cell apoptosis, transcription of TNF-α, IL-6, IL-1β and ROS production. These plant extracts markedly attenuated SA-β-gal and IL-1β and downregulated the production of IL-1α and PGE2. *In vivo*, the plant extracts dramatically dampened ROS production, the number of neutrophils, and proinflammatory cytokines. *Conclusions.* Cumulatively, this work systematically demonstrated the anti-inflammatory, antioxidant, and antisenescent properties of *Physalis alkekengi* L. and proposed the possible roles of *Physalis alkekengi* L. in inflammatory signaling pathways, providing an effective natural product for the treatment of inflammatory skin disorders.

1. Introduction

The human derma is the biggest, most extensive organ of the body that covers around $1–2 \, m^2$ area [1,2]. Derma not only regulates body temperature, and feels the touching, but also defends against the invasion of external stimuli [3]. Microscopically, the human derma appears to be orderly composed of epidermis, epidermis-dermis junction, dermis, and hypodermis from the outside in. Keratinocytes predominate in the epidermis in a well-defined manner and produce keratin associated with desmosomes to protect the skin from external attacks. The dermis includes abundant fibroblasts that release collagen and elastic fibers to the extracellular matrix (ECM) for the plasticity of skin [4, 5]. Nowadays, skin health attracts more and more people's attention with the improvement of life quality [6]. Genetic (predisposition) [7] and environmental factors (UV-radiation [8], chemical and contagious agents exposure [9, 10], and heat/cold exposure [11]) play important roles in most allergic skin diseases such as atopic dermatitis [12],

contact dermatitis [13, 14] and urticarial. Most of these allergic skin disorders are chronic, inflammatory, and proliferative [15]. The skin usually turns red, pigmented, pruritic, dry, and cracked [16] during disease development. Moreover, the interaction between chronic inflammation and senescence is attracting increasing attention [17–20]. In addition to allergic skin diseases, inflammation is closely related to pathophysiological processes in various inflammation-associated diseases such as atherosclerosis [21], acute lung injury (ALI) [22], chronic obstructive pulmonary disease (COPD) [23], periodontal disease [24] and inflammatory bowel disease (IBD) [25], which bound tightly to one another. These symptoms might deteriorate the preexisting inflammation diseases. Thus, suppressing the occurrence of skin inflammation seems to be an efficient way to relieve skin allergy, skin senescence, and inflammation-related illnesses. Hence, looking for high-performance anti-inflammatory ingredients for drugs or skincare products is considered to be a promising strategy for preventing skin diseases, aging, and inflammation-associated disorders.

Traditional natural plants are not only used as food to satisfy human necessities but also as medical and cosmeceutical ingredients [26, 27]. A huge amount of studies report numerous constituents of plant extracts possess outstanding activities such as anti-inflammation [28, 29], and antioxidation [30, 31] in vitro and in vivo. For instance, extracts of Physalis alkekengi L. [32–35], Artemisia princeps Pamp. [36], and Cannabis sativa L. [37] exhibit anti-inflammatory properties in vitro while extracts of Antarctic Lichen (Umbilicaria antarctica) [38], Soft Coral (Dendronephthya puetteri) [39], and Forsythia suspensa (Thunb.) Vahl [40] exert their anti-inflammatory abilities in vivo as well. Currently, the safety of plants gradually attracts the wide attention of scientists and consumers which could explain the popularity of natural plant extracts as functional ingredients for medicinal drugs and skincare products. Based on a large quantity of research, the total phenolic and flavonoid contents among plant extracts were identified as the functional constituents [28, 41–43]. For example, flavonoids luteolin and luteolin-7-O-glucoside derived from dandelion flowers strengthen the anti-inflammatory property and antioxidant properties in vitro [44].

Genus Physalis belongs to the Solanaceae family, distributed in Mexico, Europe, and South and Central Asia, including about 120 species [45]. Among them, Physalis alkekengi L. widely distributed in China [46, 47] is popular both in food and folk medicine as an expectorant, antitussive, diuretic, and oxytocic agents. The fruit calyces and roots of Physalis alkekengi L. used as an analgesic, antibacterial drugs, etc. in folk medicine have been reported [35]. Besides, many other pharmacological properties, including antimicrobial [48], antioxidation [49], antiapoptosis, antihyperglycemia [50], and amelioration of the side effect of cisplatin-induced nephrotoxicity [51] in vitro and in vivo have been studied. 16,24-cyclo-13,14-secosteroids named physalins have been isolated from the fruit calyces of Physalis alkekengi L. and identified since 1970 [52]. After that, dozens of physalins have been isolated [53–56]. In addition, minor metabolites such as alkaloids and flavonoids have also been identified in different parts of the plant [47, 57]. The fruit

calyces of Physalis alkekengi L. extracts (PEs) mainly contain the functional components physalins and flavonoids such as luteolin-7,4′-di-O-β-D-glucopyranoside which exhibit excellent anti-inflammatory activity in lipopolysaccharide (LPS)-induced macrophages RAW264.7 [32]. However, studies on the anti-inflammatory and antisenescent properties of PEs in human skin cells are scarce.

In this work, we collected PEs and standardized the content of flavonoids (luteolin-7,4′-di-O-β-D-glucopyranoside). The anti-inflammatory properties of PEs were tested in vitro and in vivo in two different inflammation patterns (LPS-induced and $CuSO_4$-stimulated). Levels of inflammation-associated cytokines and enzymes were evaluated not only in macrophages but also in skin cells to broaden the cosmeceutical application of PEs. Moreover, the antiaging effect of PEs was tentatively explored at a cellular level through the D-galactose (D-gal) and H_2O_2-induced fibroblast aging model to confirm the crosstalk between inflammation and cellular senescence. At last, both the anti-inflammatory and antioxidant capabilities of PEs were estimated in zebrafish embryos. The robust results of PEs in vitro and in vivo demonstrated the potential benefits of PEs for skin care.

2. Materials and Methods

2.1. Chemical.
D-galactose (D-gal), lipopolysaccharide (LPS), sodium lauryl sulfate (SLS), 2′,7′-dichlorodihydrofluorescein diacetate (H2DCFDA), copper sulfate pentahydrate ($CuSO_4 \cdot 5H_2O$) were purchased from Sigma-Aldrich (St. Louis, MO, USA). Cell-countingkit-8 (CCK-8) was obtained from Dojindo Laboratories (Japan). Quantitative real-time polymerase chain reaction (qRT-PCR) primers were purchased from Generay Biotech Co., Ltd (Shanghai, CHINA). GeneJET RNA purification kit was bought from Thermo Fisher Scientific (USA). RNA Reverse Transcription Kit was obtained from PrimeScript™ RT reagent Kit (Takara, Japan). ELISA kits were bought from NeoBioscience (Xinbosheng, China). NO assay kit, NOS kit, LDH assay kit, β-gal staining kit, and Annexin V-FITC/PI apoptosis double staining kit were purchased from Beyotime (Jiangsu, China). All chemicals were used as received without further purification.

2.2. Plant Material and Extracts Preparations.
Physalis alkekengi L. was collected from Kunming, Yunnan Province, the People's Republic of China in November 2018 and identified by Professor Haiyang Liu (based on permission No. 2018–11 from Kunming Institute of Botany, Kunming, China). Physalis alkekengi L. has been deposited in voucher specimen (No. 20181111) in the herbarium of Botany Research Institute, Shanghai Jiyan Bio-Pharmaceutical Development Co. Ltd., Shanghai, China. The part of the plant to be analyzed was thoroughly rinsed in distilled water and dried at room temperature. Collection of the fruit calyces from Physalis alkekengi L., the organization of experimental research and field research for plants (cultural or wild) was carried out in accordance with the Environmental Code of

the People's Republic of China dated April 24, 2014. The dried persistent fruit calyces of *Physalis alkekengi* L. were smashed into small pieces and put into a 250 mL flask with subsequent 95% ethanol heating reflux extraction for 2 h at 80°C. The residue was extracted another two times by the same procedure. The total extracts were collected and filtered to get rid of the undissolved residue. The combined solution was concentrated in a vacuum rotary evaporator and lyophilized immediately to obtain PEs powder. The crude extracts were stored at −80°C for the following experiments. The process of extraction was simply shown in Figure 1(a). For tested samples, PEs were dissolved in DMSO (dimethyl sulfoxide) to make a stock solution of 200 mg/mL. The stock solution was diluted using the cell culture medium for subsequent experiments *in vitro* and *in vivo*.

2.3. Analysis of Bioactive Compounds of PEs. The main bioactive compounds of PEs include bitter flavors and flavonoids. The extracts were diluted to 5 mg/mL using distilled water and analyzed by high-performance liquid chromatography (HPLC) with a referred claim in Chinese Pharmacopoeia. The effective content of luteolin-7,4′-di-O-β-D-glucopyranoside in PEs should be more than 0.42%, at which PEs exerts inflammatory activity.

2.4. Cell Culture. Immortal human keratinocyte (HaCaT), human skin fibroblast (HFF-1), and murine macrophages (RAW264.7) were bought from the Cell Bank of the Chinese Academy of Science (Shanghai, China). Cells were cultured in Dulbecco's Modified Eagle's Medium (DMEM) supplemented with 10% (v/v) fetal bovine serum at 37°C, 0.5% CO_2. HaCaT and HFF-1 were digested with 0.25% trypsin while the RAW264.7 cell line was passaged without any trypsin treatment.

2.5. Cell Viability. (a) 2×10^4 cells per well were seeded in a 96-well culture plate to reach approximately 80% confluence. No-cell wells were regarded as positive controls (PC). The culture medium was replaced by another 100 μL of complete culture medium containing different content of PEs for 24 h, and nontreatment wells were as negative controls (NC). PEs solution was substituted with 100 μL of 10% CCK-8 solution for another 2 h incubation followed by an absorbance reading taken at 450 nm. The cell survival was calculated according to the following formula: cell viability (%) = $(OD_{sample} - OD_{pc})/(OD_{nc} - OD_{pc}) \times 100\%$. Five repeats were conducted for each condition. (b) The lactate dehydrogenase (LDH) activity of cells was evaluated via an LDH assay kit. 1×10^5 cells/well were cultured in a 24-well plate for 24 h to achieve around 80% confluence, then either treated with PEs solution or not. PC was treated with the same volume of PEs-free DMEM. After 2 h incubation, H_2O_2 at 800 μM was substituted for both PEs solution and PEs-free culture medium for 2 h incubation. Then, 500 μL of complete medium replaced H_2O_2 and incubated for another 20 h. After, 200 μL of supernatant alone was harvested and mixed with 20 μL of releasing agent while the 200 μL of PC medium

together with cells were incubated with the equivalent releasing agent. 200 μL of DMEM alone mixed with 20 μL of releasing agent was as NC. Then, the solution was incubated for 1 h at 37°C, 5% CO2 and centrifuged at 1000 rpm for 4 min. 40 μL suspension per well was collected into a 96-well plate and mixed with 20 μL fresh LDH working solution that was prepared according to the manufacturer's protocol. The plate was vortexed in the dark for 30 min and the OD values were measured at 490 nm wavelength. LDH release (%) was expressed via the following equation: LDH (%) = $(OD_{sample} - OD_{nc})/(OD_{pc} - OD_{nc}) \times 100\%$. Triplicate was performed for each group.

2.6. Cell Apoptosis Assay. The percentage of early-stage apoptosis and lately-stage apoptosis, necrosis of cells induced by the addition of LPS or LPS/PEs mixture were determined through Annexin V-FITC/PI double staining assay kit (Beyotime). Cells were seeded and treated with PEs solutions together with 1 μg/mL of LPS or LPS alone. Nontreatment wells were as controls. After incubation of PEs mixed with LPS for 24 h, suspended medium (200 μL) and trypsin-disassociated cells were collected and centrifuged. The precipitate was resuspended in 195 μL of binding buffer plus 5 μL of Annexin V-FITC for 5-min incubation followed by 10-min incubation of 10 μL Propidium Iodide (PI). The nonstaining sample was as a reference. After a gentle mix at room temperature and a dark environment was conducted, the percentage of cell death was detected via Flow Cytometry (FCM). The cell plot was distributed into four quadrants based on Annexin V-FITC and PI axes representing living cells in quadrant 3, early-stage apoptotic cells in quadrant 4, and total lately-stage apoptotic and necrotic cells in quadrant 1, respectively.

2.7. Clearance of Nitric Oxide (NO) Production. 2×10^4 cells/well were seeded in a 96-well plate and incubated for 24 h. The culture medium was substituted by 100 μL of PEs solution at different concentrations or 10 μg/mL of Dexamethasone (Dex) as a positive control for 1 h, and then LPS was added to the medium directly to achieve 1 μg/mL for another 24 h incubation. The content of NO in the supernatants was detected according to the manufacturer's protocol of the Total Nitric Oxide assay kit (Beyotime).

2.8. Nitric Oxide Synthase (NOS) Assay. The activity of total NOS was detected through the NOS assay kit (Beyotime). Nonfluorescent and cell-permeable DAF-DA was esterified to weakly fluorescent DAF-FM which reacted with NO to yield fluorescent benzotriazole derivative. 2×10^4 RAW264.7 cells per well were cultured in a 96-well plate for 24 h and treated with PEs mixed with LPS for another 24 h as similar to the assay of NO production. After, the medium was replaced by 100 μL of test buffer with a subsequent 100 μL of the reaction solution. The solution mixture was cultured continuously for another 30 min. The fluorescence intensity was detected at 495 nm excitation and 515 nm emission. The Relative Fluorescence Unit (RFU) of NOS which reflects the
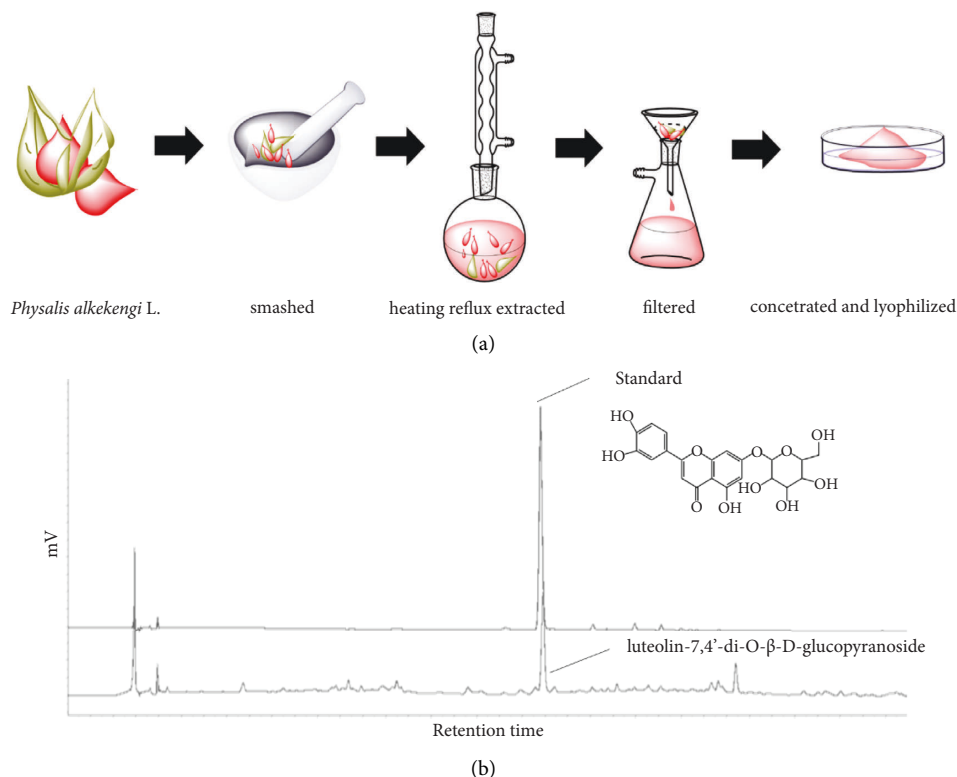
Physalis alkekengi L.   smashed   heating reflux extracted   filtered   concetrated and lyophilized

(a)

(b)

FIGURE 1: Flow chart for the extraction of *Physalis alkekengi* L. (a) and the luteolin-7,4′-di-O-β-D-glucopyranoside analyzed by HPLC (b).

activity of NOS was determined as the following equation: RFU of NOS = (RFU$_\text{treatment}$ - RFU$_\text{blank}$)/(RFU$_\text{nontreatment}$ - RFU$_\text{blank}$) where "RFU$_\text{treatment}$" means the fluorescence intensity of cells treated by PEs and LPS or LPS alone, "RFU$_\text{nontreatment}$" means the fluorescence intensity of 1×10^5 cells/well without treatment, "RFU$_\text{blank}$" represents the fluorescence intensity of buffers alone.

2.9. Enzyme-Linked Immunosorbent Assay (ELISA). 1×10^5 cells per well were seeded in 24-well for 24 h. For HFF-1, cells were pretreated with $500 \mu L$ of PEs solution at different concentrations for 2 h, then PEs solution was replaced by $400 \mu M$ of H_2O_2 for 2 h. After, cells were incubated with a freshly complete medium for another 20 h. For RAW264.7, LPS-induction was conducted according to the method of nitric oxide (NO) assay for 24 h. For HaCaT, cells were incubated with PEs at different concentrations for 12 h, then LPS was added to achieve the concentration of $10 \mu g/mL$ for another 12 h incubation. Inflammatory-associated cytokines in the supernatant were detected according to the procedure of the ELISA kit (Xinbosheng, China).

2.10. Quantitative Real-Time Polymerase Chain Reaction (qRT-PCR). 2×10^5 cells/well were seeded in a 12-well plate for 24 h. Cells were treated with LPS according to the method of ELISA. The supernatant was collected for ELISA assay while the mRNA of cell precipitate was extracted via GeneJET RNA purification kit (Thermo Scientific). The total mRNA was quantified by NanoDrop one (Thermo Scientific) and reversely transcribed using PrimeScript RT Master Mix (Takara, Shiga, Japan) according to the manufacturer's protocol ($500 \mu g$ RNA was reversely transcripted to cDNA in a final volume of $10 \mu L$). qRT-PCR was performed in a total volume of $20 \mu L$ including $10 \mu L$ of SYBR Green PCR Master Mix (Roche), $2 \mu L$ of cDNA template, and $0.4 \mu L$ of each primer ($10 \mu M$) with a Light-Cycler 96 instrument (Roche). The standard cycling conditions were 95°C for 10 min followed by 40 cycles of 95°C for 30 s and 60°C for 30 s. The ratios of the number of candidate genes to the housekeeping gene were analyzed using LightCycle 96 software to evaluate the relative mRNA levels of candidates. The sequences of primers were listed in Supplementary Table S1. Each condition was performed in triplicates.

2.11. Antioxidant Activity of PEs. 1×10^5 HaCaT cells per well were seeded in a 24-well plate for 24 h and pretreated with PEs solutions for 2 h prior to $800 \mu M$ of H_2O_2 for another 2 h. After, the level of reactive oxygen species (ROS) was quantified immediately using a ROS detection kit (Beyotime) and FCM. Briefly, cells were washed with serum-free DMEM and incubated with $1000 \times$ diluted DCFH-DA which was hydrolyzed to nonfluorescent DCFH inside the cell. ROS oxidized nonfluorescent DCFH to fluorescent DCF. The relative ROS level could be represented by the relative concentration of DCF through the fluorescence intensity of DCF detected by FCM.

2.12. *Antisenescent Activity of PEs.* Senescence-associated-β-galactosidase (SA-β-gal) activity is one of the biomarkers of cellular senescence. 5×10^4 HFF-1 cells were seeded in a 24-well plate for 24 h and incubated with PEs solution at different concentrations together with 20 mg/mL D-gal for 72 h. The enzymatic activity of cytosolic SA-β-gal was determined by in site X-gal staining kit (Beyotime). Simply, cells were washed twice with PBS and fixed for 10 min at room temperature. Then cells were washed with PBS three times (each 3 min), followed by overnight incubation of the working solution containing the substrate X-gal at 37°C in the absence of CO_2. A parafilm was used to prevent working solutions from evaporation. After, cells were further washed by PBS once and observed through an optical microscope. The number of β-gal positive cells represented the degree of cell senescence.

2.13. *Anti-Inflammatory Effect of PEs on a 3D Skin Model.* The commercial epidermal tissue EpiSkin (L'Oréal Research and Innovation Center, Shanghai, China) is an *in vitro* reconstructed human epidermis (RHE) from normal human keratinocytes cultured on a collagen matrix at the air-liquid interface. Thus, RHE is histologically similar to the *in vivo* human *epidermis* [58]. The EpiSkin models were removed from the nutrient agar and equilibrated in 12-well plates at 37°C, 5.0% CO_2 overnight. EpiSkin was irritated by 0.3% SLS, then incubated with 1 mg/mL PEs for another 20 h, nonirritated skin but still treated with PEs was a negative control. The concentration of proinflammatory factor IL-1α in the supernatant was detected by ELISA as described above. To get the UV-induced skin model, EpiSkin was exposed to the 30 J/m^3 UV for 2 h, followed by treatment of PEs for another 20 h. EpiSkin treated with PEs but not exposed to UV was used as a negative control. The content of prostaglandin E2 (PGE2) in the culture medium was measured by ELISA.

2.14. *Toxicity of PEs in Zebrafish.* The following animal experiments were reviewed and approved by The animal care and use committee of Changzhou University (ACUC NO: 20180201). We declared that all experiments and methods for the zebrafish model were performed in accordance with the internationally accepted principles for laboratory animal use and care "Animal Research: Reporting of In Vivo Experiments (ARRIVE)" guidelines. Zebrafish experiments were conducted in line with the relevant laws and the guidelines issued by the Ethical Committee. Three days postfertilization (3-dpf) zebrafish embryos were picked up at a density of ten embryos per well and incubated with PEs at different doses (0.1, 1, 10, 30, 100, 300 μg/mL) for 24 h at 28°C. The percent survival of zebrafish was directly determined through observation under bright-field microscopy.

2.15. *Antioxidant Effect of PEs on Zebrafish.* Quantification of ROS in Zebrafish was determined by the cell-permeable fluorescent probe H2DCFDA. H2DCFDA is hydrolyzed

inside the cell to nonfluorescent probe CM-H2DCFDA which could be oxidized by ROS to fluorescent dye DCF. The fluorescence intensity of DCF reflects the oxidative stress of the cell. Thirty zebrafish embryos (3-dpf) per group were selected and treated either with PEs at different concentrations (30, 100 μg/mL) or not for 24 h at 28°C. Zebrafish embryos were washed twice and incubated with 20 μg/mL H2DCFDA for 1 h in the dark. After, embryos were anesthetized with 0.0003% MS-222 (tricaine methane-sulfonate) and subsequently observed through a fluorescence microscope. The average fluorescent intensity of the individual group was quantified using SpectraMax i3x Multimode microplate reader and calculated through Image J. Group treated with 3 mg/mL of Tripeptide-1 was used as a positive control (PC).

2.16. *Anti-Inflammatory Effect on Zebrafish.* Ten 3-dpf transgenic zebrafish embryos with neutrophil-specific fluorescence: Tg (mpx: dsRED) were chosen and exposed to 1 μM of $CuSO_4$ either alone or together with 30 or 100 μg/mL PEs for 2 h at 28°C. The embryos without $CuSO_4$ treatment were used as a negative control. After the development and fluorescence intensity of zebrafish embryos were observed by fluorescence microscope, in the meanwhile, the number of neutrophils was counted by image J. Anti-inflammatory activity of PEs was represented by the reduced percentage of neutrophils.

2.17. *qRT-PCR in Zebrafish.* Thirty 3-dpf zebrafish embryos per group were stimulated by 1 μM $CuSO_4$ as written in the method "Anti-inflammatory effect on zebrafish". The total RNA was extracted from zebrafish embryos through RNA-Quick Purification Kit (ES Science) following the manufacturer's instructions. RNA was dissolved and reverse-transcribed into cDNA. The following qRT-PCR for the measurement of five oxidation- and inflammation-associated genes expression were conducted as described in the above method of qRT-PCR. The details of primers were given in Supplementary Table S2. All conditions were performed in triplicates.

2.18. *Data Statistics.* Data were represented as the mean ± standard of at least two independent repeated experiments done in duplicate or triplicate. Differences were considered at NS, $p > 0.05$, $^*p < 0.05$, $^{**}p < 0.01$, $^{***}p < 0.001$, $^\#p < 0.05$, $^{\#\#}p < 0.01$, and $^{\#\#\#}p < 0.001$ using a two-tailed Student's t-test.

3. Results and Discussion

3.1. *Quantification of Luteolin-7,4'-di-O-β-D-glucopyranoside in PEs.* The fruit calyces of *Physalis alkekengi* L. were extracted according to the procedure described in Figure 1(a). Lyophilized PEs were dissolved in DMSO and analyzed by high-performance liquid chromatography (HPLC). The highest peak in Figure 1(b) was verified according to the retention time and a spike with a standard

of luteolin-7,4'-di-O-β-D-glucopyranoside. The effective peak area was completely separated from other compositions and reached 0.42%, which was well suited to the claim of Chinese Pharmacopoeia.

3.2. Anti-Inflammatory Property of PEs in LPS-Stimulated RAW264.7 Cells

3.2.1. Inhibition of NO and Nitric Oxide Synthase (NOS) Production by PEs in LPS-Stimulated RAW264.7 Cells. The effective concentrations of PEs were determined through a well-known model of LPS-induced inflammation in RAW264.7 murine macrophage. LPS is a major component of the Gram-negative bacterial cell wall that induces inflammation through known TLR4-MyD88 signaling [59, 60]. The inflammatory repertoire of the culture medium is initially evaluated with regard to the level of NO production. Figure 2(a) showed that 10 μg/mL of PEs slightly eliminates the formation of NO while 50 μg/mL of PEs significantly attenuates 60% of NO production, exceeding that of positive control dexamethasone (Dex). Besides, noncytotoxicity of PEs below 100 μg/mL was observed. We subsequently studied the total NOS activity of PEs at the effective concentrations of 50, 100, and 200 μg/mL. Figure 2(b) suggested PEs entirely suppressed the enzyme activities while Dex only had a slight inhibition of NOS activity. These results elucidated that PEs exhibited excellent anti-inflammatory properties in vitro. LPS-stimulated inflammation could further contribute to cell death. Since PEs shows great potential for anti-inflammatory agents, we would like to explore the protection of PEs from cell apoptosis. As Figure 2(c) showed, PEs presented a good protective effect against LPS-induced apoptosis in a dose-dependent way.

3.2.2. Inhibition of Differentiation in LPS-Stimulated RAW264.7 Cells. We then examined the protection of PEs against LPS-induced morphology changes by using microscopy. The bright-field microscope images in Figure S1 indicated that 1 μg/mL LPS induced the small round-shaped RAW264.7 into an elongated shape of dendritic filopodia, while both 50 μg/mL and 100 μg/mL PEs limited cell differentiation. In addition, 100 μg/mL PEs alone did not make any influence on the cell compared to the group of NC.

3.2.3. Anti-Inflammatory Mechanism of PEs. To further explore the anti-inflammatory mechanism involved in the treatment of PEs, we investigated the expression levels of two well-known proinflammatory factors interleukins (ILs) IL-6 and IL-1β cell-secreted in the supernatant of LPS-induced RAW264.7. The plot in Figure 3(a) indicated that LPS-induced 800-fold-higher levels of IL-6 production than that in the negative control, 100 μg/mL of PEs inhibited approximately 50% of LPS-induced IL-6 expression. Similarly, Figure 3(b) suggested that 100 μg/mL PEs totally down-regulated the expression of IL-1β to a normal level. By the way, treatment of PEs alone would not make any effect on the

proinflammatory factors production. Inflammation and cellular senescence have been connected directly through ILs-dependent inflammatory networks [61]. Taking into consideration that ILs production was greatly inhibited by PEs above, PEs may take part in antisenescence as well. Matrix metalloproteinase-9 (MMP-9) is expressed in the intracellular and extracellular matrix, maintaining the construction of intercellular collagen and fibers. Moreover, MMP-9 belonging to the member of senescence-associated secretory phenotypes (SASPs) plays a role not only in the signaling pathway of inflammation but also in cell senescence. Figure 3(c) showed that LPS extremely promoted the expression of MMP-9 while 100 μg/mL PEs dramatically reduced 50% of MMP-9 expression. These results further revealed the anti-inflammatory properties and the antiaging potential of PEs. Furthermore, we investigated the mRNA levels of inflammation-related factors through high-sensitivereal-time fluorescent quantitative PCR (qRT-PCR). In Figure 3(d)–3(k), LPS-stimulation resulted in a significant increase in the transcription activities of several proinflammatory cytokines (IL-6, IL-10, IL-α, and IL-1β) and TNF-α mRNA, while 50–100 μg/mL of PEs performed a significant decrease in the levels of them. That provided more evidence for the anti-inflammatory effect of PEs. Moreover, gene levels of important mediators of inflammation, NOS, cyclooxygenase-2 (COX-2), and the metabolic prostaglandin E2 (PGE2) were down-regulated through PEs incubation compared with non-PEs incubation in response to LPS-stimulation. The details of PCR primer pair sequences were given in Supplementary Information Table S1.

3.3. Effects of PEs on Human Keratinocyte (HaCaT)

3.3.1. Alleviation of LPS-Induced Cytotoxicity by PEs in Human Keratinocyte HaCaT. The anti-inflammatory property of PEs has been demonstrated in the LPS-induced inflammatory model of murine macrophages. Thus, we explored whether PEs could be used in skincare products since sensitive skin could secret large quantities of proinflammatory factors when encountering allergens. To investigate the protective ability of PEs against LPS-induced injury in human epidermal cells HaCaT, we studied the cytotoxicity of PEs at different concentrations for 12 h, 24 h, and 36 h incubation, respectively. As shown in Supporting Information Figure S2, PEs at concentrations of up to 100 ng/mL caused no cytotoxicity within 24 h incubation while showing non-negligible toxicity at 36 h incubation in HaCaT. Bright-field microscopy images of cell morphological changes treated by PEs in Figure S3(a) confirmed the safety of PEs incubation at concentrations below 100 ng/mL for 24 h. We further analyzed the protective effect of PEs at 25, 50, and 100 ng/mL. Figure S3(b) indicated that PEs concentration-dependently reduced the LPS-induced cell damage.

3.3.2. Anti-Inflammation of PEs in Human Keratinocyte HaCaT. Additionally, PEs exerted anti-inflammatory activity in HaCaT skin cells as well. Consequently, PEs at the
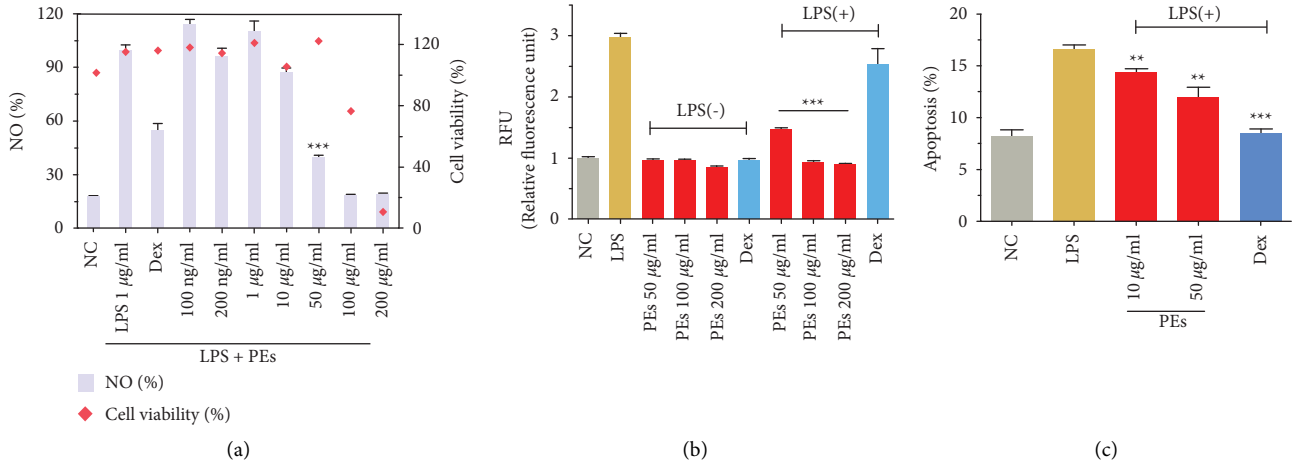
(a)

(b)

(c)

Figure 2: Quantification of NO production and cell viability (a), NOS activities (b), and cell apoptosis (c) in RAW264.7. PEs at different concentrations were incubated with cells for 1 h prior to incubation with LPS (1 μg/mL) for 24 h. Treatment of LPS plus Dex at 10 μg/mL was a positive control. Each experiment was conducted in triplicate. Significant differences from the LPS-treated group were regarded as $^{**}p < 0.01$, $^{***}p < 0.001$.
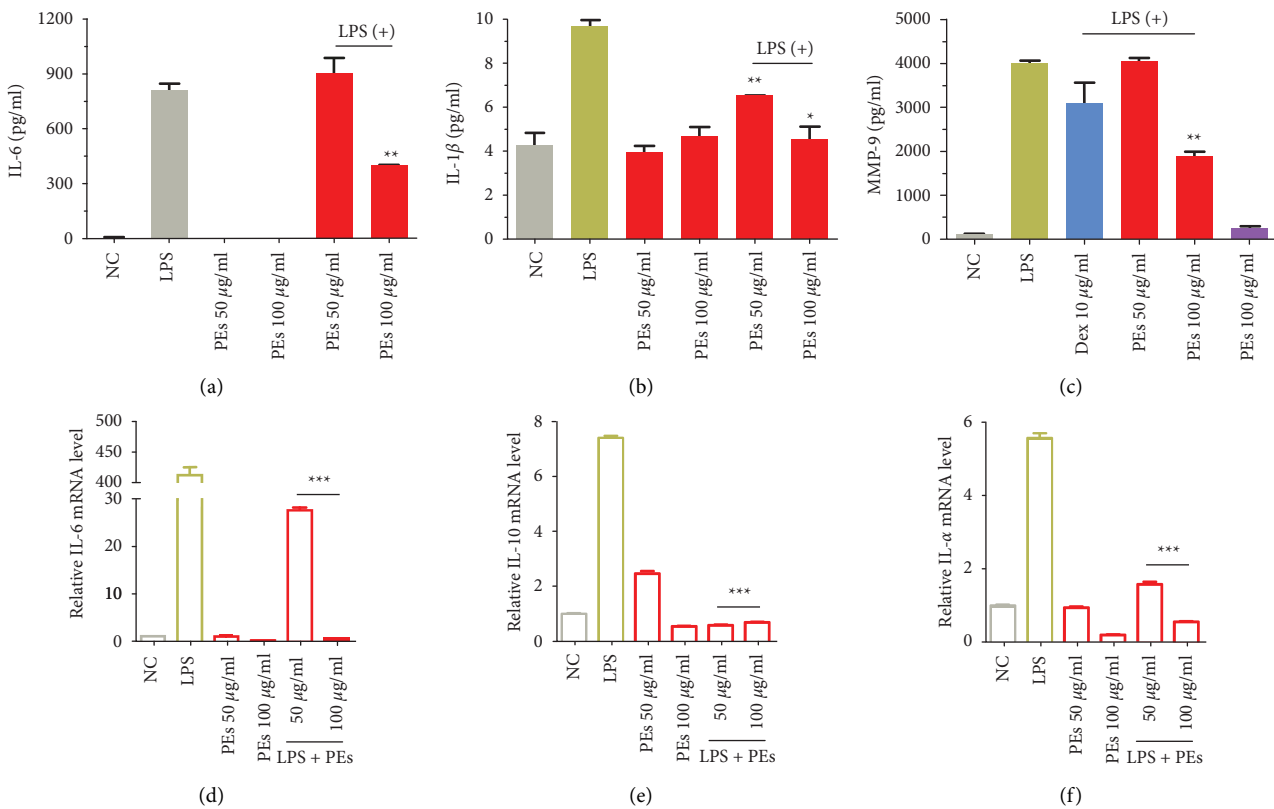

(a)

(b)

(c)

(d)
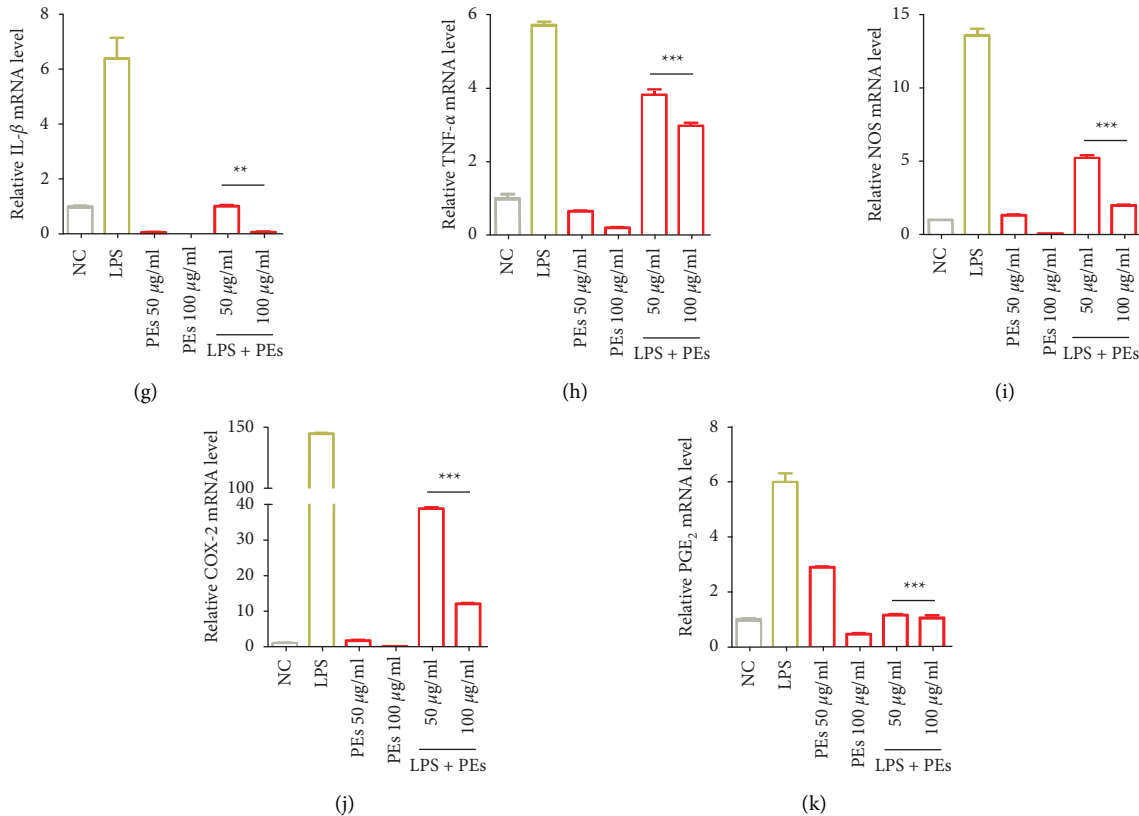
(e)

(f)

Figure 3: Continued.

(g)

(h)

(i)

(j)

(k)

Figure 3: Anti-inflammatory effects of PEs on LPS-stimulated RAW264.7. Cells were pretreated with PEs at the concentrations of 50, 100 μg/mL for 1 h and exposed to 1 μg/mL LPS for another 24 h. After, IL-6 (a), IL-1β (b), and MMP-9 (c) production in the cell culture supernatant were detected by using an enzyme-linked immunosorbent assay (ELISA). The cells were collected and lysed for the measurement of the relative expression of genes involved in immune responses (IL-6 (d), IL-10 (e), IL-α (f), IL-1β (g), TNF-α (h), NOS (i), COX-2 (j), and PGE2 (k)) by qRT-PCR analysis (β-Actin expression was used as an internal control). Each experiment was performed in triplicate. $^{*}p < 0.05$, $^{**}p < 0.01$, $^{***}p < 0.001$ compared to the group of LPS-treatment alone.

range of concentrations (25–100 ng/mL) down-regulated the mRNA levels of inflammatory-related factors TNF-α, IL-6, and IL-1β shown in Figure S4 which further indicated the anti-inflammatory function of PEs and implied the possibilities of PEs for allergic skincare products.

3.3.3. Antioxidant Activity of PEs in Human Keratinocyte HaCaT.

The relationship between inflammation and oxidative stress is interdependent [62]. Oxidative stress develops in the site of inflammation due to the production of reactive species (ROS) and further promotes inflammation, while the secretion of proinflammatory factors eventually accentuates oxidative stress. Inhibition of ROS could be a way to attenuate inflammation. We evaluated the antioxidant properties of PEs in HaCaT cells through quantitative measurement of ROS formation. Here, the oxidative damage model was implemented through a well-established H_2O_2-induced cell injury [63]. The result in Figure S5(a) showed PEs at concentrations higher than 500 ng/mL could effectively reduce H_2O_2-induced oxidative stress. The protective effect of PEs from H_2O_2-induced damage has also been proven by endogenous lactate dehydrogenase (LDH) release assay in Figure S5(b), 100 ng/mL of PEs could

prevent around 15% of H_2O_2-induced LDH release. Taken together, PEs exhibited both anti-inflammatory and antioxidant properties in HaCaT.

3.4. Anti-senescent Activity of PEs in Human Skin Fibroblast (HFF-1).

The excellent performance of PEs in anti-inflammation in RAW264.7 and oxidation-resistance in keratinocytes HaCaT shed new light on the role of PEs in antisenescence treatments since a number of antiaging ingredients exhibit well antioxidant activity. We explored the antiaging ability of PEs in the second passage of infant foreskin fibroblast HFF-1. Senescence-associatedβ-galactosidase (SA-β-gal) is the most widely used biomarker of aging which could be overexpressed in senescent cells and diseased tissues [64]. D-gal induces rat or cell-aged models which is similar to natural aging for the study of senescent mechanism [65, 66]. D-gal was first used in an aging inducer by Chinese researchers in 1985. It was reported that injections of D-gal shorten the longevity in mice [65], drosophila [67], and human fetal lung fibroblast [68]. Although the exact aging mechanism of D-gal remains unclear, the possible mechanism is that, on the one hand, D-gal is a reducing sugar that exists naturally in the body,

however, excessive D-gal could be oxidized into aldose and hydrogen peroxide through galactose oxidase, leading to the production of ROS [69] which subsequently cause oxidative stress, senescence, inflammation and apoptosis [70]; on the other hand, D-gal reacts with the free amines of amino acids in proteins and peptides to form advanced glycation end-products (AGEs) which are associated with senescence, diabetes, Alzheimer's disease [65]. Figure 4(a) showed treatment only with D-gal extremely increased the percentage of SA-β-gal positive cells that could be inhibited through coadministration with 100 ng/mL of PEs. Statistical analysis in Figure 4(b) suggested that almost 90% of the antisenescent activity of PEs at 100 ng/mL. In addition, IL-1β in the HFF-1 culture medium treated by PEs was quantified in Figure 4(c), which was significantly lower than that of H_2O_2-induced. These results suggested PEs made an effect on inhibition of skin senescence and inflammation, to some extent providing evidence for the link between inflammation and aging [17] and showing the prospects of PEs in skin care.

3.5. Anti-Inflammation of PEs in Reconstituted Skin Model.

A reconstituted skin model is used to mimic dermal tissue and implies the potential role of PEs in allergic skin diseases. We used the well-established sensitive skin models: sodium lauryl sulfate (SLS)-irritated and UV-radiated models to detect the anti-inflammatory activities of PEs [71–73]. Figure S6 showed PEs decreased proinflammatory factor IL-1α mRNA expression more efficiently than that of positive control Dex from SLS-irritation, indicating an improvement of PEs in allergic skin. Sunlight exposure is also one of the frequent ways to encounter allergic skin and then get skin inflammation. Here, 30 J/cm^3 of UV irradiation was used to prepare an allergic skin model. Both PEs could comparably inhibit PGE2 mRNA production compared with the non-treatment control. These results shed light on the anti-inflammation of PEs in derma mimics, which directed the possibilities of PEs' application in skin care.

3.6. Effects of PEs on Zebrafish.

Zebrafish models have been widely used in developmental biology and drug discovery because of their low maintenance costs, transparency, and high similarity to human genomes [74, 75]. The oxidant and inflammatory models could be easily and robustly constructed and visualized in zebrafish. The copper-induced inflammatory response has been used widely because it is noninvasive compared with physical damage-induced inflammation [76, 77].

3.6.1. Antioxidant Effect of PEs on Zebrafish.

The toxicity of PEs at different concentrations in zebrafish embryos was determined by microscopy after 24 h incubation. Figure 5(a) showed that PEs at concentrations of up to 100 μg/mL has negligible toxicity on the survival rate of zebrafish embryos while 300 μg/mL of PEs led to total mortality of zebrafish embryos. Hence, we treated zebrafish embryos with 30 μg/mL and 100 μg/mL of PEs for the following antioxidation and anti-inflammation assays. The ROS level after PEs incubation was quantified by using a fluorescence probe. The fluorescent microscopy images of zebrafish embryos in Figure 5(b) suggested fluorescence intensity significantly decreased in the presence of PEs at 100 μg/mL compared with that in the nontreatment group. The bright-field microscopy indicated PEs incubation made no difference to the survival of zebrafish embryos. The fluorescence intensity is graphed in Figure 5(c), both 30 μg/mL and 100 μg/mL PEs evidently limited the generation of ROS *in vivo*, demonstrating the profound antioxidant effect of PEs. Furthermore, heat shock proteins (Hsp) are crucial families in protecting the cell against damage from oxidative stress. Interestingly, Figure S7 *further revealed PEs at the indicated concentrations protected zebrafish embryos against oxidative damage from CuSO$_4$ through the down-regulation of a stress-related gene Hsp70.*

3.6.2. Anti-Inflammatory Effect of PEs on Zebrafish.

The crosstalk between oxidative stress and inflammation mentioned before reminds us to study the anti-inflammatory property of PEs as well in zebrafish. Accumulation of serum copper levels that trigger oxidative stress responses and activate inflammatory responses in a dose-dependent manner. CuSO$_4$-induced inflammatory responses would activate, macrophages and recruit neutrophils [78]. Therefore, the anti-inflammatory property of PEs was evaluated by monitoring the number of red-fluorescence labeled neutrophils in a neutrophil-specific transgenic zebrafish model Tg (mpx: dsRED). The red-fluorescence intensity would increase resulting from CuSO$_4$. Figure 6(a) indicated the tested concentration of PEs. The fluorescent microscopy images in Figure 6(b) revealed that coadministration with PEs at the indicated doses obviously reduced the number of red fluorescent-labeled neutrophils from the CuSO$_4$ alone administration, meaning the alleviation of inflammation. Figure 6(c) suggested PEs at 100 μg/mL decreased by around 67% of the number of neutrophils compared with the treatment of CuSO$_4$ alone. We subsequently quantified the levels of inflammation-related genes (Primer was listed in Table S2). *However, Figures 6(d)–6(g) suggested after CuSO$_4$ exposure, PEs at 100 μg/mL excellently downregulated the levels of IL-6, complement C3a, and phospholipase A2 (PLA2) mRNA, which are involved in MAPK-mediated inflammatory signaling pathway.*

4. Discussion

The human derma is an important organ for protecting the human body from the invasion of external stimuli. Nowadays, people are more concerned about the appearance of the skin. Most skin disorders are chronic and inflammatory, which result in superficial skin changes and produce crosstalk with other pathophysiological processes. Moreover, inflammatory cytokines are members of senescence-associated secretory phenotypes (SASPs) secreted through senescent cells, meaning inflammatory response might accelerate the development of senescence. Thus, inhibition of
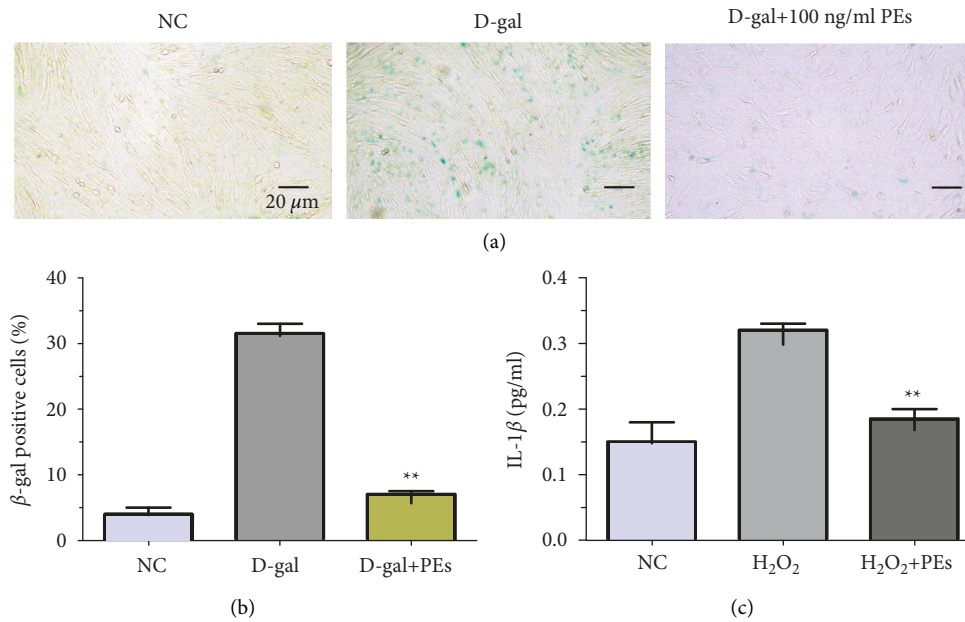
(a)

(b)

(c)

FIGURE 4: Antisenescent effect of PEs on HFF-1. Cells were treated with 20 mg/mL of D-gal together with 100 ng/mL of PEs for 72 h. After, cells were stained according to the manufacturer's protocol. β-gal positive cells (in blue) were observed through microscopy (scale bar represents 20 μm) (a) and counted (b), moreover, the anti-inflammatory effect of PEs on HFF-1 was evaluated according to the ELISA experiment of IL-1β in cell culture medium after treatment with 400 μM of H_2O_2 with/without 100 ng/mL PEs (c). Each experiment was performed in triplicate. ** $p < 0.01$ compared to the groups of D-gal- or H_2O_2-treatment.
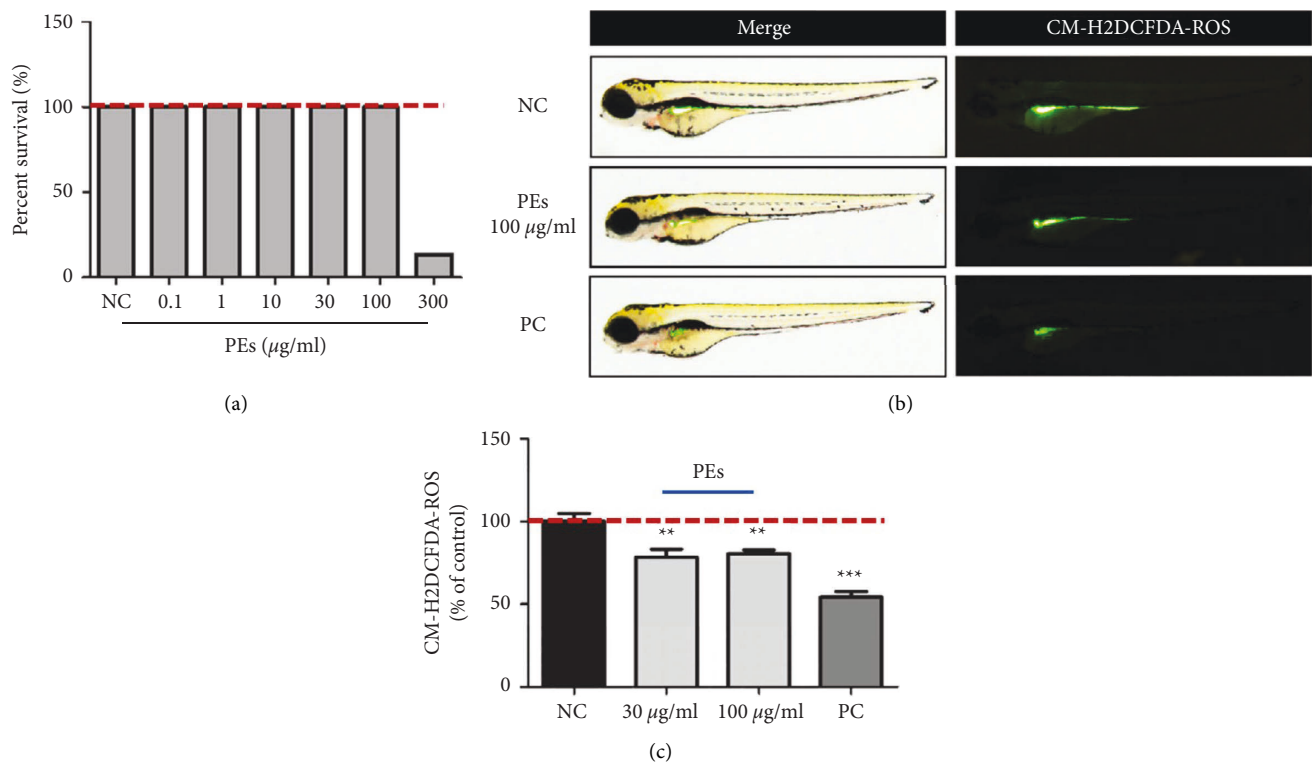

(a)

(b)

(c)

FIGURE 5: Antioxidant effect of PEs in vivo. Thirty zebrafish embryos were incubated either with PEs at different concentrations or Tripeptide-1 as the positive control (PC) for 24 h. After, toxicity in zebrafish embryos was determined through bright-field microscopy while the ROS levels were detected through a fluorescent dye H2DCFDA. Briefly, 20 μg/mL of H2DCFDA replaced the PEs to incubate with embryos for 1 h in the dark. After washing three times, the fluorescence was observed via fluorescence microscopy (c) and the fluorescence intensity was obtained using a microplate reader (b). ** $p < 0.01$, *** $p < 0.001$ compared to the nontreatment group.
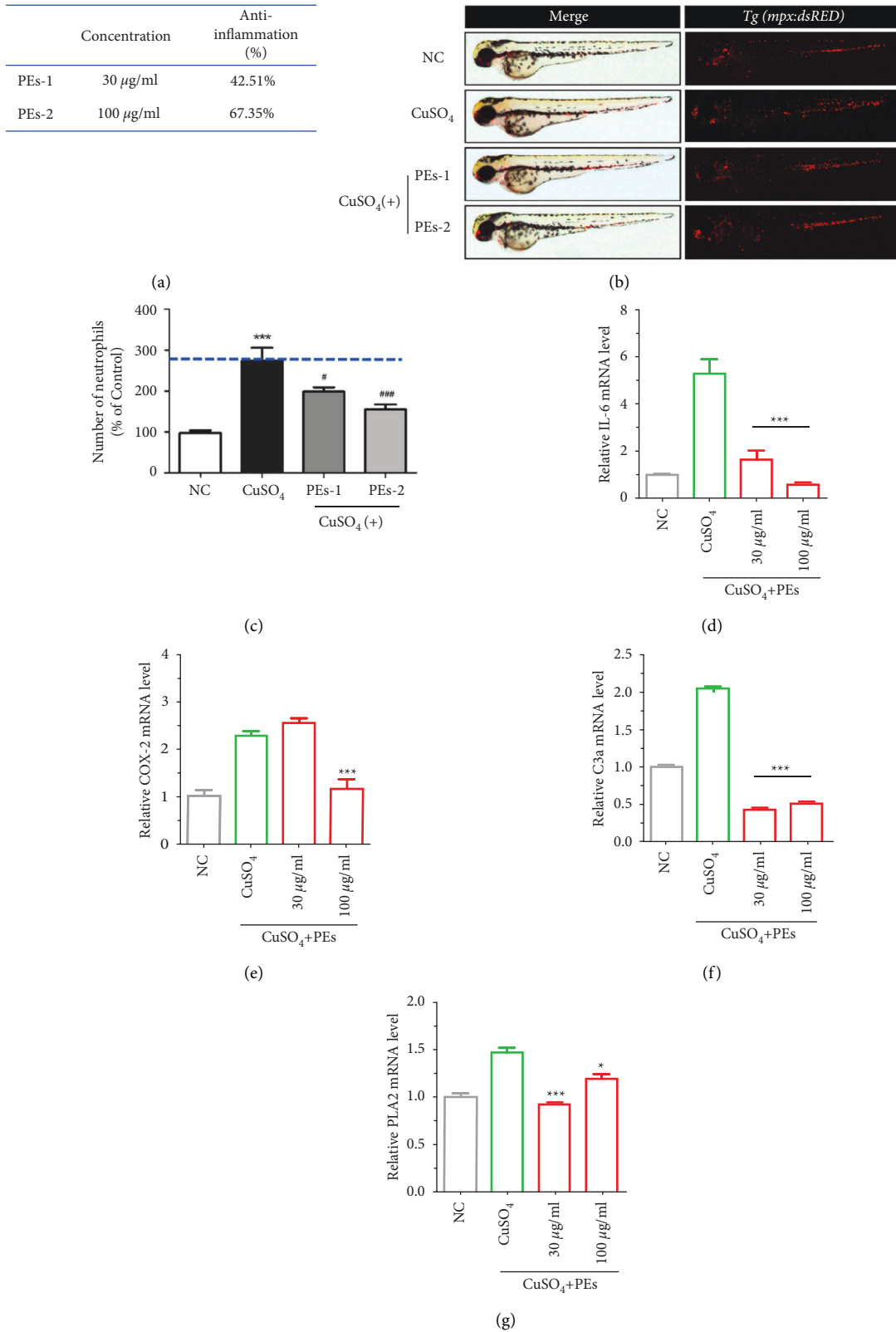
	Concentration	Anti-inflammation (%)
PEs-1	30 μg/ml	42.51%
PEs-2	100 μg/ml	67.35%

(a)

(b)

(c)

(d)

(e)

(f)

(g)

FIGURE 6: Anti-inflammatory effect of PEs against $CuSO_4$-induced inflammation *in vivo*. (a) Effective concentrations of PEs and anti-inflammatory efficacies. (b) The fluorescence images of zebrafish embryos after treatment with 1 μM $CuSO_4$ alone or together with PEs at different concentrations. (c) The number of neutrophils in transgenic zebrafish embryos under different treatment conditions, $***p < 0.001$ compared with the nontreatment group, and $^{#}p < 0.05$, $^{###}p < 0.001$ compared with the group treated with $CuSO_4$ alone (a-c). The expression of inflammation-related genes (IL-6, COX-2) and eicosanoid pathway-associated genes (COX-2, C3a, and PLA2) *in vivo*. The zebrafish embryos were exposed to $CuSO_4$ either with PEs or not for 2h. After, embryos were collected for qRT-PCR analysis. A pool of 30 embryos per group was used. Experiments were performed in triplicates. $*p < 0.05$, $***p < 0.001$ compared to the experiment treated with $CuSO_4$ alone (d-g).
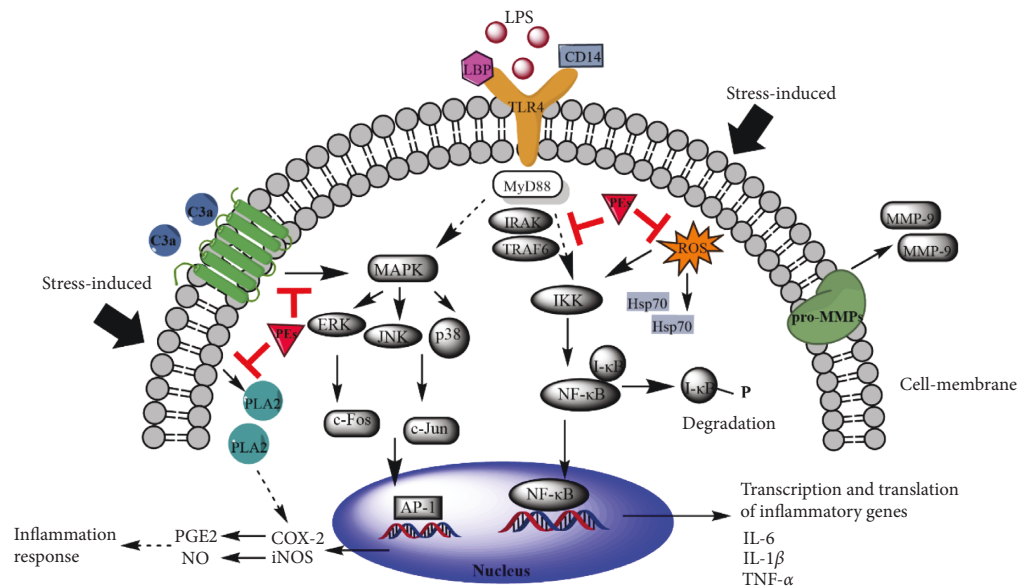
Figure 7: Proposed roles of PEs in the suppression of LPS-induced and oxidative stress-induced inflammatory pathways.

skin inflammation seems to be an alternative way to cure skin disorders, aging, and inflammation-related illness. Traditional natural plants have been considered desirable candidates for medical and cosmeceutical ingredients because of their safety and efficacy *in vitro* and *in vivo*. *Physalis alkekengi* L. belongs to the Solanaceae family distributed widely in China and is popular both in food and folk medicine. However, the anti-inflammatory activity of *Physalis alkekengi* L. extracts (PEs) has been most exhibited in immune cells, the studies of the anti-inflammatory and antisenescent activities of PEs in human skin cells remain scarce.

Our study showed the protective effects of PEs from LPS-induced damage through inhibition of inflammation-related enzymes and gene expression not only in murine macrophage RAW264.7 but also in one skin cell line, keratinocyte HaCaT. Interestingly, PEs also attenuated the expression of senescence-associated marker SA-β-gal and proinflammatory factor IL-1β in skin fibroblast cells HFF-1 induced by D-gal and H_2O_2, which to some extent emphasized the interdependent relationship between inflammation and aging. Importantly, the study also initiatively illustrated the anti-inflammatory properties of PEs in SLS-stimulated and UV-radiated 3D reconstructed human skin models for allergy research, implying the impact of PEs on allergic skin diseases. Here, *in vivo* anti-inflammation of PEs has also been demonstrated in the copper-sulfate-induced zebrafish embryos model. These robust results provided a strong basis for the promising application of PEs in the fields of anti-inflammatory medicine and cosmetics.

With respect to the mechanisms of PEs in response to inflammation and oxidative stress, we envisaged the possible roles of PEs in the anti-inflammatory and antioxidant pathways in Figure 7. Taken together, LPS molecules together with LPS binding protein (LBP) bound to CD14 were transferred to toll-like receptor 4 (TLR4)-MyD88 complex to

initiate the inflammatory pathways, although the exact roles of LBP and CD14 in the recognition of LPS remain elusive. MAPK and IKK, the downstream proteins of MyD88 were activated in the subsequent MAPK/AP-1 and IKK/NF-κB signaling with the production of proinflammatory cytokines such as IL-6, IL-1β, and TNF-α. As for the stimuli of oxidative stress, on the one hand, oxidative stress from the treatment of H_2O_2 or copper sulfate increased the generation of intracellular ROS to activate the NF-κB signaling, on the other hand, stress-activated the metabolizing enzymes such as phospholipase A2 (PLA2) and COX-2 for the degradation of membrane lipids to a final product PGE2. Therefore, oxidative damage exacerbated the inflammation response. On the basis of the study, PEs directly reduced the ROS levels, which partly inhibited the NF-κB signaling. Moreover, PEs might suppress MAPK-mediated inflammation through the down-regulation of PLA2 and complement C3a levels. However, further studies are required to interpret whether the expression of mRNA is consistent with the production of corresponding proteins due to transcriptional and post-translational modifications. Furthermore, pieces of evidence are needed to identify the exact targets of PEs in the anti-inflammatory pathways and the roles of PEs (besides inhibition of MMP-9) in cell senescence which could broaden the application of PEs in skin care products.

5. Conclusions

In summary, this work showed the anti-inflammatory and antioxidant effects of traditional herbal medicines PEs *in vitro* and *in vivo*. More importantly, this paper explored the antisenescent activity of PEs through suppression of SASPs which revealed, to some extent, the relationship between inflammation and senescence. In the end, we illustrated the possible roles of PEs in two main inflammation-related signaling pathways, as summarized in

Figure 7. Accordingly, the robust data shed light on PEs as a promising anti-inflammatory and antisenescent ingredient in skincare-associated products. However, further studies are needed to isolate the biologically functional compounds involved in PEs and identify the exact targets to evaluate their activities.

Data Availability

All data generated or analyzed during this study are included in this published article. Raw data are available from the corresponding author upon reasonable request.

Ethical Approval

Zebrafish experiments were conducted in line with the relevant laws and the guidelines issued by the Ethical Committee.

Conflicts of Interest

The authors declare that there are no conflicts of interest regarding the publication of this paper.

Authors' Contributions

Li-Ping Qu contributed to the study conception and design. Data collection and manuscript preparation were conducted by Bing-Wei He. The final version of the manuscript was directed and modified by Fei-Fei Wang and Li-Ping Qu. All authors discussed and approved the final manuscript.

Supplementary Materials

Table S1. primers used to analyze the expression of inflammatory genes in RAW264.7. Table S2. Primers used to analyze the expression of inflammatory genes in zebrafish. Figure S1: bright-field microscopy images of RAW264.7 treated by PEs at 50, $100 \mu g/mL$ for 1 h prior to incubation with LPS ($1 \mu g/mL$) for 24 h. Treatment of LPS plus Dex at $10 \mu g/mL$ was a positive control while incubation of PEs at $100 \mu g/mL$ alone was a negative control. The scale bar represents $20 \mu m$. Figure S2: cytotoxicity of PEs at various concentrations for 12, 24, and 36 h incubation in keratinocytes HaCaT. Cell viability was measured by MTT assay. Three independent experiments (triplicate for each) were performed. $^{**}p < 0.01$ compared to the nontreatment group. Figure S3: protective effect of PEs from LPS-damage on HaCaT. Cells were incubated either with PEs alone at different does or not for 24 h, then observed using bright-field microscopy (a). Cells were incubated with PEs for 12 h prior to treatment with $10 \mu g/mL$ of LPS for another 12 h. Then, cell viability was measured via MTT assay (b). Triplicate was done for each experiment group. $^{*}p < 0.05$, $^{**}p < 0.01$ compared to the LPS-induced group while $^{##}p < 0.01$ compared to control. The scale bar represents $20 \mu m$. Figure S4: anti-inflammatory effects of PEs on TNF-α (a), IL-6(b), and IL-1β (c) expression in LPS-induced HaCaT culture medium using enzyme-linked immunosorbent assay (ELISA). Cells were treated with PEs at the concentrations of 25, 50, and $100 \mu g/mL$ for 12 h before incubation with LPS ($10 \mu g/mL$) for another 12 h. Triplicate was conducted in the experiments. $^{**}p < 0.01$ compared to the cells treated with LPS alone, $^{##}p < 0.01$ compared with control. Figure S5: antioxidant effect of PEs on HaCaT. Cells were pretreated with PEs at different concentrations for 2 h, then incubated with $800 \mu M$ of H_2O_2 for another 2 h. The level of reactive oxygen species (ROS) was quantified immediately using a membrane-permeable probe DCFH-DA and flow Cytometry (FCM) (a). The cytotoxicity of PEs at $100 ng/mL$ in HaCaT was measured through LDH release as well (b) Triplicate was conducted in the experiments. $^{*}p < 0.05$, $^{**}p < 0.01$, $^{***}p < 0.001$ compared to the cells treated with H_2O_2 alone. Figure S6: anti-inflammation effect of PEs on IL-1α (a) and PGE2 (b) in SLS-irritated or UV-radiated 3D skin models using enzyme-linked immunosorbent assay (ELISA). The skin was transferred into a 6-well plate and treated either with 0.3% SLS or $30J/cm^3$ UV for 2 h, followed by $1 mg/mL$ of PEs or Dex incubation for another 20 h. $^{***}p < 0.001$, $^{****}p < 0.0001$, compared to the non-SLS- and non-UV-stimulated skin but still treated with PEs or Dex. Figure S7: the expression of the antioxidant gene (Hsp70) *in vivo*. Thirty zebrafish embryos were exposed to $CuSO_4$ either with PEs or not for 2 h. After, embryos were collected for qRT-PCR analysis. Experiments were performed in triplicates. $^{***}p < 0.001$ compared to the experiment treated with $CuSO_4$ alone. (*Supplementary Materials*)

References

[1] M. Leider and C. M. Buncke, "Physical dimensions of the skin; determination of the specific gravity of skin, hair, and nail," *AMA archives of dermatology and syphilology*, vol. 69, no. 5, pp. 563–569, May 1954.

[2] L. Ringham, P. Prusinkiewicz, and R. Gniadecki, "Skin patterning in psoriasis by spatial interactions between pathogenic cytokines," *iScience*, vol. 20, pp. 546–553, 2019.

[3] C. M. Chuong, B. J. Nickoloff, P. M. Elias et al., "What is the 'true' function of skin?" *Experimental Dermatology*, vol. 11, no. 2, pp. 159–187, Apr. 2002.

[4] C. Hwa, E. A. Bauer, and D. E. Cohen, "Skin biology," *Dermatologic Therapy*, vol. 24, no. 5, pp. 464–470, 2011.

[5] L. Celleno and F. Tamburi, "Chapter 1 - structure and function of the skin," in *Nutritional Cosmetics*William Andrew Publishing, New York USA, 2009.

 [6] J. Lehtimäki, H. Sinkko, A. Hielm-Björkman et al., "Skin microbiota and allergic symptoms associate with exposure to environmental microbes," in *Proceedings of the National Academy of Sciences of the United States of America*, vol. 115, no. 19, pp. 4897–4902, May 2018.

 [7] N. Morar, S. A. G. Willis-Owen, M. F. Moffatt, and W. O. C. M. Cookson, "The genetics of atopic dermatitis," *The Journal of Allergy and Clinical Immunology*, vol. 118, no. 1, pp. 24–34, 2006.

 [8] C. R. Taylor and A. J. Sober, "Sun exposure and skin disease," *Annual Review of Medicine*, vol. 47, no. 1, pp. 181–191, 1996.

 [9] J. P. Thyssen, E. Giménez-Arnau, J.-P. Lepoittevin, T. Menne, A. Boman, and A. Schnuch, "The critical review of methodologies and approaches to assess the inherent skin sensitization potential (skin allergies) of chemicals Part II," *Contact Dermatitis*, vol. 66, no. s1, pp. 25–52, 2012.

[10] S. Kezic and J. B. Nielsen, "Absorption of chemicals through compromised skin," *International Archives of Occupational and Environmental Health*, vol. 82, no. 6, pp. 677–688, 2009.

[11] T. V. Kozyreva and G. M. Khramova, "Effects of activation of skin ion channels TRPM8, TRPV1, and TRPA1 on the immune response. Comparison with effects of cold and heat exposure," *Journal of Thermal Biology*, vol. 93, Article ID 102729, 2020.

[12] J. Fenner and N. B. Silverberg, "Skin diseases associated with atopic dermatitis," *Clinics in Dermatology*, vol. 36, no. 5, pp. 631–640, 2018.

[13] D. Slodownik, A. Lee, and R. Nixon, "Irritant contact dermatitis: a review," *Australasian Journal of Dermatology*, vol. 49, no. 1, pp. 1–11, 2008.

[14] K. E. Andersen, C. Benezra, D. Burrows et al., "Contact dermatitis," *Contact Dermatitis*, vol. 16, no. 2, pp. 55–78, 1987.

[15] A. W. Ho and T. S. Kupper, "T cells and the skin: from protective immunity to inflammatory skin disorders," *Nature Reviews Immunology*, vol. 19, no. 8, pp. 490–502, 2019.

[16] O. A. Olusegun and B. S. Martincigh, "Allergic contact dermatitis: a significant environmental and occupational skin disease," *International Journal of Dermatology*, vol. 60, no. 9, pp. 1082–1091, 2021.

[17] A. Freund, A. V. Orjalo, P.-Y. Desprez, and J. Campisi, "Inflammatory networks during cellular senescence: causes and consequences," *Trends in Molecular Medicine*, vol. 16, no. 5, pp. 238–246, 2010.

[18] T. Tchkonia, Y. Zhu, J. van Deursen, J. Campisi, and J. L. Kirkland, "Cellular senescence and the senescent secretory phenotype: therapeutic opportunities," *Journal of Clinical Investigation*, vol. 123, no. 3, pp. 966–972, Mar. 2013.

[19] J. Campisi, "Aging, cellular senescence, and cancer," *Annual Review of Physiology*, vol. 75, no. 1, pp. 685–705, 2013.

[20] L. Ferrucci and E. Fabbri, "Inflammageing: chronic inflammation in ageing, cardiovascular disease, and frailty," *Nature Reviews Cardiology*, vol. 15, no. 9, pp. 505–522, 2018.

[21] P. Libby, Y. Okamoto, V. Z. Rocha, and E. Folco, "Inflammation in atherosclerosis: transition from theory to practice," *Circulation Journal*, vol. 74, no. 2, pp. 213–220, 2010.

[22] R. B. Goodman, J. Pugin, J. S. Lee, and M. A. Matthay, "Cytokine-mediated inflammation in acute lung injury," *Cytokine & Growth Factor Reviews*, vol. 14, no. 6, pp. 523–535, 2003.

[23] M. J. Sevenoaks and R. A. Stockley, "Chronic Obstructive Pulmonary Disease, inflammation and co-morbidity – a common inflammatory phenotype?" *Respiratory Research*, vol. 7, no. 1, p. 70, 2006.

[24] A. Cekici, A. Kantarci, H. Hasturk, and T. E. Van Dyke, "Inflammatory and immune pathways in the pathogenesis of periodontal disease," *Periodontology*, vol. 64, no. 1, pp. 57–80, 2014.

[25] R. J. Xavier and D. K. Podolsky, "Unravelling the pathogenesis of inflammatory bowel disease," *Nature*, vol. 448, no. 7152, pp. 427–434, 2007.

[26] L. C. Tapsell, I. Hemphill, L. Cobiac et al., "Health benefits of herbs and spices: the past, the present, the future," *Medical Journal of Australia*, vol. 185, no. S4, pp. S1–S24, Aug. 2006.

[27] F. Jamshidi-Kia, Z. Lorigooini, and H. Amini-Khoei, "Medicinal plants: past history and future perspective," *Journal of Herbmed Pharmacology*, vol. 7, no. 1, pp. 1–7, Jan. 2018.

[28] P. Diaz, S. C. Jeong, S. Lee, C. Khoo, and S. R. Koyyalamudi, "Antioxidant and anti-inflammatory activities of selected medicinal plants and fungi containing phenolic and flavonoid compounds," *Chinese Medicine*, vol. 7, no. 1, p. 26, 2012.

[29] S. Kumar and A. K. Pandey, "Chemistry and biological activities of flavonoids: an overview," *Science World Journal*, vol. 2013, Article ID 162750, 2013.

[30] Z. A. M. Yasin, F. Ibrahim, N. N. Rashid, M. F. M. Razif, and R. Yusof, "The importance of some plant extracts as skin anti-aging resources: a review," *Current Pharmaceutical Biotechnology*, vol. 18, no. 11, pp. 864–876, 2018.

[31] X. Li, A. Zhou, and Y. Han, "Anti-oxidation and anti-microorganism activities of purification polysaccharide from Lygodium japonicum in vitro," *Carbohydrate Polymers*, vol. 66, no. 1, pp. 34–42, 2006.

[32] J.-M. Hong, O.-K. Kwon, I.-S. Shin et al., "Anti-inflammatory activities of Physalis alkekengi var. franchetii extract through the inhibition of MMP-9 and AP-1 activation," *Immunobiology*, vol. 220, no. 1, pp. 1–9, 2015.

[33] Z. Shu, N. Xing, Q. Wang et al., "Antibacterial and anti-inflammatory activities of Physalis alkekengi var. franchetii and its main constituents," *Evid. Based Complement. Alternat. Med.* vol. 2016, Article ID 4359394, 2016.

[34] H. I. F. Magalhães, M. R. Torres, L. V. Costa-Lotufo et al., "In-vitro and in-vivo antitumour activity of physalins B and D from Physalis angulata," *Journal of Pharmacy and Pharmacology*, vol. 58, no. 2, pp. 235–241, 2010.

[35] H. Kang, S.-R. Kwon, and H.-Y. Choi, "Inhibitory effect of *Physalis alkekengi* L. var. franchetii extract and its chloroform fraction on LPS or LPS/IFN-γ-stimulated inflammatory response in peritoneal macrophages," *Journal of Ethnopharmacology*, vol. 135, no. 1, pp. 95–101, 2011.

[36] K.-R. Park, Y. Jeong, J. Lee, I. K. Kwon, and H.-M. Yun, "Anti-tumor effects of jaceosidin on apoptosis, autophagy, and necroptosis in human glioblastoma multiforme," *American Journal of Cancer Research*, vol. 11, no. 10, pp. 4919–4930, 2021.

[37] T. Nuutinen, "Medicinal properties of terpenes found in Cannabis sativa and Humulus lupulus," *European Journal of Medicinal Chemistry*, vol. 157, pp. 198–228, 2018.

[38] J.-M. Hong, J. E. Kim, S. K. Min et al., "Anti-inflammatory effects of antarctic lichen umbilicaria Antarctica methanol extract in lipopolysaccharide-stimulated RAW 264.7 macrophage cells and zebrafish model," *BioMed Research International*, vol. 2021, pp. 1–12, 2021.

[39] E.-A. Kim, Y. Ding, H.-W. Yang, S.-J. Heo, and S.-H. Lee, "Soft coral dendronephthya puetteri extract ameliorates inflammations by suppressing inflammatory mediators and oxidative stress in LPS-stimulated zebrafish," *International Journal of Molecular Sciences*, vol. 19, no. 9, p. 2695, 2018.

[40] L. Gong, L. Yu, X. Gong et al., "Exploration of anti-inflammatory mechanism of forsythiaside A and forsythiaside B in CuSO(4)-induced inflammation in zebrafish by metabolomic and proteomic analyses," *Journal of Neuroinflammation*, vol. 17, no. 1, p. 173, Jun. 2020.

[41] R. A. Mustafa, A. A. Hamid, S. Mohamed, and F. A. Bakar, "Total phenolic compounds, flavonoids, and radical scavenging activity of 21 selected tropical plants," *Journal of Food Science*, vol. 75, no. 1, pp. C28–C35, 2010.

[42] N. Saeed, M. R. Khan, and M. Shabbir, "Antioxidant activity, total phenolic and total flavonoid contents of whole plant extracts Torilis leptophylla L," *BMC Complementary and Alternative Medicine*, vol. 12, no. 1, p. 221, 2012.

[43] C. D. Stalikas, "Extraction, separation, and detection methods for phenolic acids and flavonoids," *Journal of Separation Science*, vol. 30, no. 18, pp. 3268–3295, 2007.

[44] C. Hu and D. D. Kitts, "Luteolin and luteolin-7-O-glucoside from dandelion flower suppress iNOS and COX-2 in RAW264.7 cells," *Molecular and Cellular Biochemistry*, vol. 265, no. 1/2, pp. 107–113, 2004.

[45] N. Sharma, A. Bano, H. Dhaliwal, and V. Sharma, "A pharmacological comprehensive review on 'rassbhary' *physalis angulata*(L.)," *International Journal of Pharmacy and Pharmaceutical Sciences*, vol. 7, pp. 34–40, Jun. 2015.

[46] M. Vessal, H. A. Mehrani, and G. Hossein Omrani, "Effects of an aqueous extract of Physalis alkekengi fruit on estrus cycle, reproduction and uterine creatine kinase BB-isozyme in rats," *Journal of Ethnopharmacology*, vol. 34, no. 1, pp. 69–78, 1991.

[47] K. Basey, B. A. McGaw, and J. G. Woolley, "Phygrine, an alkaloid from Physalis species," *Phytochemistry*, vol. 31, no. 12, pp. 4173–4176, 1992.

[48] S. Helvaci, G. Kökdil, M. Kawai, N. Duran, G. Duran, and A. Guvenc, "Antimicrobial activity of the extracts and physalin D from Physalis alkekengi and evaluation of antioxidant potential of physalin D," *Pharmaceutical Biology*, vol. 48, no. 2, pp. 142–150, Feb. 2010.

[49] M. Moniruzzaman, Y.-W. Chin, and J. Cho, "HO-1 dependent antioxidant effects of ethyl acetate fraction from Physalis alkekengi fruit ameliorates scopolamine-induced cognitive impairments," *Cell Stress & Chaperones*, vol. 23, no. 4, pp. 763–772, 2018.

[50] L. G. Vicas, T. Jurca, I. Baldea et al., "*Physalis alkekengi* L. Extract reduces the oxidative stress, inflammation and apoptosis in endothelial vascular cells exposed to hyperglycemia," *Molecules*, vol. 25, no. 16, p. 3747, 2020.

[51] S. Changizi-Ashtiyani, M. Alizadeh, H. Najafi et al., "Physalis alkekengi and Alhagi maurorum ameliorate the side effect of cisplatin-induced nephrotoxicity," *Cancer Gene Therapy*, vol. 23, no. 7, pp. 235–240, 2016.

[52] T. Matsuura, M. Kawai, R. Makashima, and Y. Butsugan, "Structures of physalin A and physalin B, 13, 14-seco-16, 24-cyclo-steroids from Physalis alkekengi var. Francheti," *Journal of the Chemical Society, Perkin Transactions 1*, vol. 5, pp. 664–670, 1970.

[53] L. R. Row, K. S. Reddy, N. S. Sarma, T. Matsuura, and R. Nakashima, "New physalins from Physalis angulata and Physalis lancifolia. Structure and reactions of physalins D, I, G and K," *Phytochemistry*, vol. 19, no. 6, pp. 1175–1181, 1980.

[54] M. Kawai, T. Matsuura, S. Kyuno et al., "A New physalin from Physalis alkekengi: structure of physalin L," *Phytochemistry*, vol. 26, no. 12, pp. 3313–3317, 1987.

[55] B. Makino, M. Kawai, K. Kito, H. Yamamura, and Y. Butsugan, "New physalins possessing an additional carbon-bond from Physalis alkekengi var. francheti," *Tetrahedron*, vol. 51, no. 46, pp. 12529–12538, 1995.

[56] M. Kawai, T. Yamamoto, B. Makino et al., "The Structure of Physalin T from *Physalis alkekengi* var.*francheti*," *Journal of Asian Natural Products Research*, vol. 3, no. 3, pp. 199–205, 2001.

[57] M. F. Ramadan and J.-T. Mörsel, "Analysis of glycolipids from black cumin (*Nigella sativa* L.), coriander (*Coriandrum sativum* L.) and Niger (*Guizotia abyssinica Cass.*) oilseeds," *Food Chemistry*, vol. 80, no. 2, pp. 197–204, 2003.

[58] H. Kandárová, M. Liebsch, E. Schmidt et al., "Assessment of the skin irritation potential of chemicals by using the SkinEthic reconstructed human epidermal model and the common skin irritation protocol evaluated in the ECVAM skin irritation validation study," *Alternatives to Laboratory Animals*, vol. 34, no. 4, pp. 393–406, 2006.

[59] A. Poltorak, X. He, I. Smirnova et al., "Defective LPS signaling in C3H/HeJ and C57BL/10ScCr mice: mutations in Tlr4 gene," *Science*, vol. 2822088 pages, 1998.

[60] K. Hoshino, O. Takeuchi, T. Kawai et al., "Cutting edge: toll-like receptor 4 (TLR4)-deficient mice are hyporesponsive to lipopolysaccharide: evidence for TLR4 as the Lps gene product," *The Journal of Immunology*, vol. 162, no. 7, pp. 3749–3752, 1950.

[61] G. Tsirpanlis, "Cellular senescence and inflammation: a noteworthy link," *Blood Purification*, vol. 28, no. 1, pp. 12–14, 2009.

[62] S. K. Biswas, "Does the interdependence between oxidative stress and inflammation explain the antioxidant paradox?" *Oxidative Medicine and Cellular Longevity*, vol. 2016, Article ID 5698931, 2016.

[63] M. Giorgio, M. Trinei, E. Migliaccio, and P. G. Pelicci, "Hydrogen peroxide: a metabolic by-product or a common mediator of ageing signals?" *Nature Reviews Molecular Cell Biology*, vol. 8, no. 9, pp. 722–728, 2007.

[64] G. P. Dimri, X. Lee, G. Basile et al., "A biomarker that identifies senescent human cells in culture and in aging skin in vivo," in *Proceedings of the National Academy of Sciences of the United States of America*, vol. 92, no. 20, pp. 9363–9367, 1995.

[65] X. Song, M. Bao, D. Li, and Y. M. Li, "Advanced glycation in d-galactose induced mouse aging model," *Mechanism of Ageing and Development*, vol. 108, no. 3, pp. 239–251, 1999.

[66] K. F. Azman and R. Zakaria, "d-Galactose-induced accelerated aging model: an overview," *Biogerontology*, vol. 20, no. 6, pp. 763–782, 2019.

[67] X. Cui, L. Wang, P. Zuo et al., "D-Galactose-caused life shortening in *Drosophila melanogaster* and *Musca domestica* is associated with oxidative stress," *Biogerontology*, vol. 5, no. 5, pp. 317–326, 2004.

[68] X. Cui, W. Li, and B. Zhang, "Studies on cell senescence induced by D-galactose in cultured neurons and fibroblasts," *Zhongguo ying yong sheng li xue za zhi = Zhongguo yingyong shenglixue zazhi = Chinese journal of applied physiology*, vol. 13, no. 2, pp. 131–133, 1997.

[69] W.-S. Wu, J.-R. Wu, and C.-T. Hu, "Signal cross talks for sustained MAPK activation and cell migration: the potential role of reactive oxygen species," *Cancer & Metastasis Reviews*, vol. 27, no. 2, pp. 303–314, 2008.

[70] H.-U. Simon, A. Haj-Yehia, and F. Levi-Schaffer, "Role of reactive oxygen species (ROS) in apoptosis induction," *Apoptosis*, vol. 5, no. 5, pp. 415–418, 2000.

[71] D. Xian, X. Xiong, J. Xu et al., "Nrf2 overexpression for the protective effect of skin-derived precursors against UV-

induced damage: evidence from a three-dimensional skin model," *Oxidative Medicine and Cellular Longevity*, vol. 2019, Article ID 7021428, 2019.

[72] D. Jírová, D. Basketter, M. Liebsch et al., "Comparison of human skin irritation patch test data with in vitro skin irritation assays and animal data," *Contact Dermatitis*, vol. 62, no. 2, pp. 109–116, 2010.

[73] T. Yonezawa, R. Momota, H. Iwano et al., "Unripe peach (Prunus persica) extract ameliorates damage from UV irradiation and improved collagen XVIII expression in 3D skin model," *Journal of Cosmetic Dermatology*, vol. 18, no. 5, pp. 1507–1515, 2019.

[74] K. Stoletov, V. Montel, R. D. Lester, S. L. Gonias, and R. Klemke, "High-resolution imaging of the dynamic tumor cell–vascular interface in transparent zebrafish," *Proceedings of the National Academy of Sciences*, vol. 104, no. 44, pp. 17406–17411, 2007.

[75] S. Ali, H. G. J. v. Mil, and M. K. Richardson, "Large-scale assessment of the zebrafish embryo as a possible predictive model in toxicity testing," *PLoS One*, vol. 6, no. 6, Article ID e21076, 2011.

[76] P. M. Craig, C. M. Wood, and G. B. McClelland, "Oxidative stress response and gene expression with acute copper exposure in zebrafish (*Danio rerio*)," *American Journal of Physiology - Regulatory, Integrative and Comparative Physiology*, vol. 293, no. 5, pp. R1882–R1892, 2007.

[77] A. Johnson, E. Carew, and K. A. Sloman, "The effects of copper on the morphological and functional development of zebrafish embryos," *Aquatic Toxicology*, vol. 84, no. 4, pp. 431–438, 2007.

[78] D. M. Mosser and J. P. Edwards, "Exploring the full spectrum of macrophage activation," *Nature Reviews Immunology*, vol. 8, no. 12, pp. 958–969, 2008.